The interaction of polymer dispersed liquid crystal sensors with ultrasound

View Online   Export Citation   CrossMark

R. S. Edwards,[a] (iD) J. Ward, L. Q. Zhou, (iD) and O. Trushkevych[a] (iD)

AFFILIATIONS

Department of Physics, University of Warwick, Coventry, CV4 7AL, United Kingdom

[a]Authors to whom correspondence should be addressed: r.s.edwards@warwick.ac.uk and o.trushkevych@warwick.ac.uk

ABSTRACT

Polymer dispersed liquid crystals (PDLCs) have been shown to be sensitive to ultrasound through the acousto-optic effect. The acousto-optic response of PDLCs was studied over a broad frequency range (0.3–10 MHz). We demonstrate that the displacements required to produce acousto-optic clearing of PDLC films can be as low as a few nanometers, which is at least 10^3 times smaller than the PDLC droplet size, is 10^5 times smaller than the PDLC layer thickness, and of the order of the molecular size of the liquid crystal constituents. This suggests that the acousto-optic effect in PDLCs is due to the microscopic effects of the LC reorientation under torques or flows rather than the LC reorientation through macroscopic droplet deformation. The displacement required for clearing is related to the frequency of operation via an exponential decay. We attribute the observed frequency response to a freezing out of the rotational motion around the short axis of the liquid crystal. The reported frequency dependence and displacements required indicate that the effects and materials described here could be used for ultrasound visualization in a non-destructive testing context.

Liquid crystals (LCs) are sensitive to ultrasound fields.[1–6] In 1971, Mailer *et al.* studied the birefringence of an aligned LC layer using a 10 MHz ultrasound transducer.[2] This acousto-optic effect has been used to develop acoustography for non-destructive testing (NDT), whereby a thick, aligned layer of LCs can be used to image ultrasound after it has passed through a sample in a water bath, identifying defects within the sample.[1,7] Recently, ultrasound has been used to control the orientation in a LC cell with periodic patterns observed in the optical behavior,[3,4] with a variable focus lens developed.[5]

A LC-based sensor that was flexible and could operate outside of a water bath and without polarizers would bring many benefits. For this, polymer-dispersed LCs (PDLCs) could be used.[8,9] In such materials, droplets of LCs are suspended in a polymer matrix, with the refractive index of the matrix chosen to match those of the LCs in their aligned state. In the unaligned state, the film scatters light, whereas as the LCs in the droplets are aligned, the film becomes clear. Changes in alignment can therefore be seen visually without the requirement for polarizers.[10]

The acousto-optic effect in aligned LC films is fairly well understood, but the underlying mechanisms are still debated.[6,11–13] The mechanism of the interaction of ultrasound with PDLCs is less clear. Several researchers have reported that ultrasound will clear PDLC films, with clearing of the whole film due to leaky wavemodes from a surface acoustic wave reported in Refs. 14 and 15. We have recently shown the visualization of acoustic fields using PDLC films, demonstrated by the clearing of a film on top of an air-coupled ultrasound transducer, with the cleared regions matching the regions of the largest amplitude vibration during resonance for frequencies below 1 MHz.[16]

In order to build a PDLC-based ultrasound sensor, it is essential to quantify the sensitivity and ensure that it is suitable for typical ultrasound displacements used in fields such as NDT. Similar work has been performed for the driving of the clearing using an electric field, studying the saturation voltage and threshold required for clearing.[17] A full understanding of clearing must consider the ultrasonic displacement, the frequency range of operation, and the clearing efficiency over this range. Ultrasound frequencies from tens of kHz to tens of MHz are used for NDT, depending on the application. This paper studies the behavior of a PDLC sensor on an air-coupled ultrasound transducer over a wide range of frequencies. It is tempting to use excitation voltage for the air-coupled transducer directly; however, there is not necessarily a linear correlation between excitation voltage and displacement for an ultrasound transducer, and the relationship varies depending on the position of the transducer and the mode shape.[18,19] Instead, the displacement was measured using an interferometer, while the clearing as a function of displacement was quantified through photography and image analysis.

A 25 mm diameter flexural ultrasound transducer was used, which is composed of a piezoelectric element glued onto an aluminum cap.[21] These are designed to operate at low frequencies (fundamental resonance around 50 kHz) and will also resonate at higher frequencies for higher-order modes. The transducer was driven by a continuous sine wave using a function generator with a 25 W RF power amplifier. The excitation voltage was varied to change the displacement of the cap surface. Imaging of two low frequency modes (the 6:0 axi-symmetric mode close to 300 kHz and the 11:0 axi-symmetric mode around 730 kHz) using both the laser vibrometer and PDLC sensor was presented in Ref. 16.

The transducer was coated with a thin layer of pink UV-curable varnish, to ensure good optical contrast when observing clearing. The PDLC films were produced using E7 and Norland adhesive NOA68, at a concentration of 75% LC, drop-cast onto the varnish layer, and covered with a glass slide with spacers to form a 100 μm thick film. NOA68 is a UV curable adhesive and has been shown to produce a good sensor for ultrasound when used with a high concentration of E7.[14,16] The LC droplet size distribution was analyzed using polarized optical microscopy. For this, a 25 μm film was produced using the same preparation parameters as for the 100 μm films; the thinner film was less scattering and allowed detailed microscopic images to be acquired for analysis.

The setup of the transducer and PDLC is shown in the inset of Fig. 1. Impedance analysis showed that adding the varnish and PDLC layers on top of the transducer changed its resonant frequencies by 5%. Displacement measurements had to be done on the transducer without the PDLC and top cover, and this was later taken into account when locating resonant frequencies. Ultrasound signals were generated for transducer resonant frequencies between 300 kHz and 10 MHz, with driving voltages of between 50 mVpp and 250 mVpp pre-amplifier.

Prior to the application of the PDLC layer, the transducer was characterized. Figure 1 shows the displacement measured at the center of the transducer using an Intelligent Optical Systems two-wave mixer interferometer, with a bandwidth of 250 MHz, for an excitation voltage of 100 mVpp. Note that the measurement at just this position will not identify all modes but only those with significant displacement at the center. Many resonances are shown by the peaks, with optimal generation at frequencies below 3 MHz. Above 3 MHz, several small amplitude peaks are observed, corresponding to higher order modes.
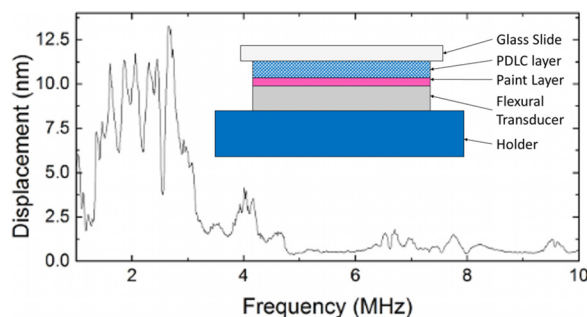
Figure 2(a) shows the displacement measured during a one-dimensional (line) scan across the center of the transducer, plotted as a color scale as a function of excitation voltage, at a frequency of 0.29 MHz. Note that the magnitude of the displacement at each point has been plotted, and hence, both the peaks and dips are the maxima. At low excitation voltages, the expected mode shape is observed. As the voltage is increased above 200 mV, the central peak shows a splitting, indicative of non-linear behavior.[18,19] Part (b) shows the displacement at the central point of the transducer plotted over the reduced excitation voltage range where linearity is observed in (a). The transducer shows two regions of behavior, above and below 50 mV. All clearing measurements have therefore been done for voltages between 50 and 200 mVpp, and hence, one linear region can be used for transducer calibration. Further characterisation of the transducer displacements was done for all modes studied using the PDLC sensor. All measurements were performed over the main linear region of the displacement vs voltage curve.

The PDLC film structure was studied using polarized microscopy. The films were strongly polydisperse, and the droplets were not always spherical. It should be noted that the film thickness acts as a low pass filter for droplet size, and extrapolating droplet size distribution in the 100 μm film from studying a 25 μm thick film will not account for droplets with sizes above 25 μm. National Instruments software package Vision Builder AI & Visual Studio was used to analyze droplet size distributions on a micrograph with a ×10 objective lens. This magnification gave a good depth of field and allowed a large number of droplets to be visible at the same time. The inset of Fig. 3 shows that good recognition of droplets was achieved. However, some droplets were merged or slightly out of focus, giving an over- or under-estimation of the droplet area in some cases. The largest number of droplets was under 4 μm in diameter, with a large population of droplets of 4–20 μm in diameter (Fig. 3). The larger droplets dominate the occupied volume.

Photographs were taken at each voltage during clearing for different resonance modes using a DSLR camera (Canon EOS 600D). Care was taken to ensure that lighting conditions were identical for each photograph, with the aperture of f/6.3 and shutter speed, and an ISO of 800 being kept constant. Before each sequence of photographs taken, the PDLC film was pre-warmed,[16] ensuring that the PDLC response time was sufficiently short to take photographs with a stabilization time of only a few seconds. The time step between changing the
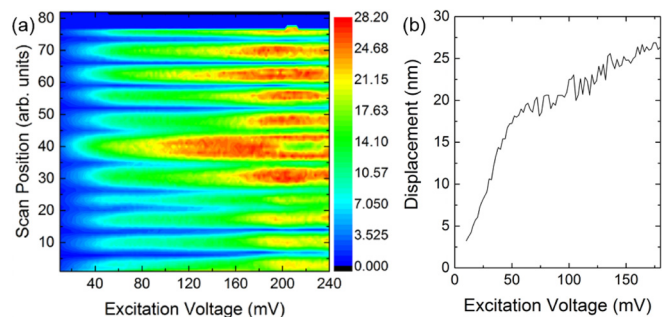

FIG. 1. Displacement of the air-coupled transducer for an excitation voltage of 100 mVpp, measured at the center, omitting the fundamental frequency. The inset shows the setup once the PDLC film has been applied.

FIG. 2. (a) Color plot of displacement during a scan across the center of the transducer. (b) Displacement for the resonance. Both are measured for the mode at 0.29 MHz.
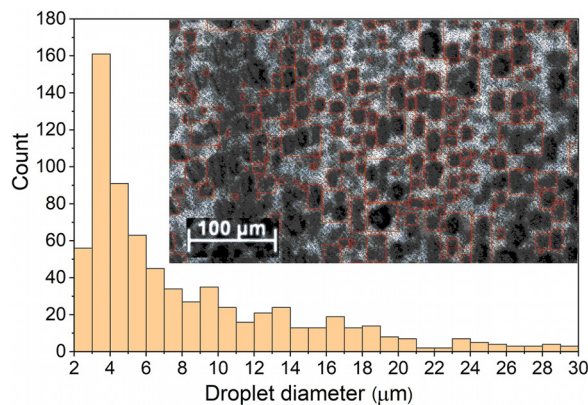
FIG. 3. PDLC structure for a 25 μm film, showing the calculated droplet diameter distribution; the inset shows droplet size analysis using Vision Builder AI from a polarized microscopy image.

FIG. 5. (a) Ratios calculated from the photographs, showing clearing, as a function of displacement. (b) Displacement at 50% clearing. The insets show thermal images taken at two of the frequencies at 50% clearing.

driving voltage and taking the photograph was kept constant. Figures 4(a)–4(c) show several modes measured over a frequency range of 0.29–9.65 MHz, showing the broadband nature of the sensor; note that minor image processing has been applied for print quality. The low frequency resonances shown in (a) and (b) correspond to full vibrational motion of the aluminum cap. The smaller diameter displacement regions at the highest frequencies, such as that shown in (c), correspond primarily to the vibration of the piezoelectric active element passing through the cap, as these are well above the standard operational frequency range for the cap.

Figures 4(e)–4(g) show the clearing of the mode at 2.17 MHz for several excitation voltages; note that again image processing has only been used to make these clear for printing. At low excitation voltages, the mode clearing is not visible to the eye. As the excitation voltage is increased, the resonant mode shape becomes distinct, until by a driving voltage of 200 mVpp, and the energy input is enough to initiate thermal clearing.

Image analysis was used to quantify the changes in behavior. To allow for any variation in lighting between different photographs in a sequence, photographs were turned into greyscale and the analysis used the ratio between the greyscale value in a region where the PDLC film clears [blue box in Fig. 4(c)] and that of a reference region, taken away from the PDLC film (red box). The calculated ratio plotted against measured displacement is shown for several modes in Fig. 5(a). The data show a very small initial rise, indicating that the PDLC film becomes more scattering; this is not visible to the eye and might be due to the onset of the molecular reorientation in LC
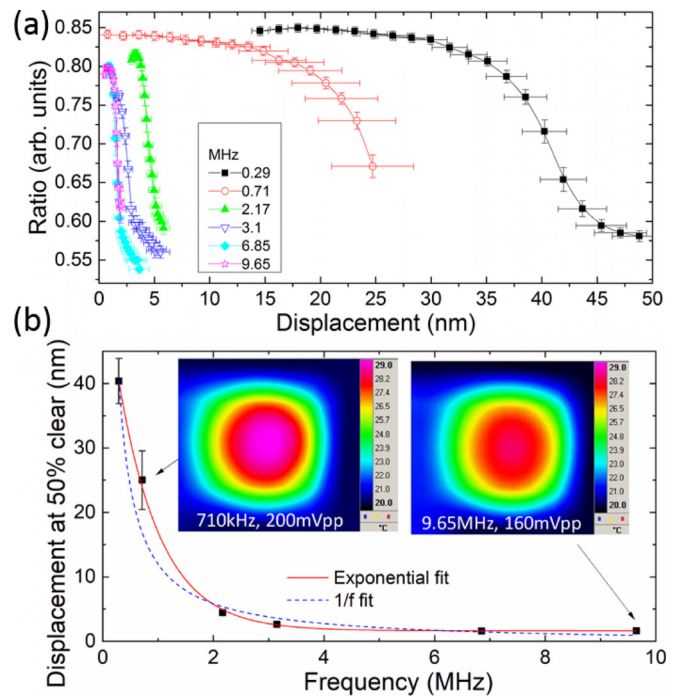
droplets. After this brief rise, the ratio drops, indicating the onset of clearing, before it is visible to the eye. Beyond a particular driving voltage, the ratio levels off, indicating that the PDLC is saturated (fully cleared). All measurements were done, while the mode shape was clear, keeping away from the thermal clearing regime.

The heating of piezoelectric transducers occurs and increases with excitation power and frequency.[20] Raised temperatures increase the sensitivity of PDLC films to ultrasound.[16] The temperature of the transducer surface was monitored using a Cedex Titanium 20 thermal camera. A transducer with a paint layer was covered with black tape with known emissivity. The transducer was excited with voltages that are sufficient to obtain the acousto-optic effect at the reported frequencies. The temperature rise was very similar for all resonant modes studied, with heating to around 28 °C for all modes [shown as the insets of Fig. 5(b)], enabling the direct comparison of results from different frequencies. The observed clearing is not due to a thermal transition into the isotropic phase because it is observed when the
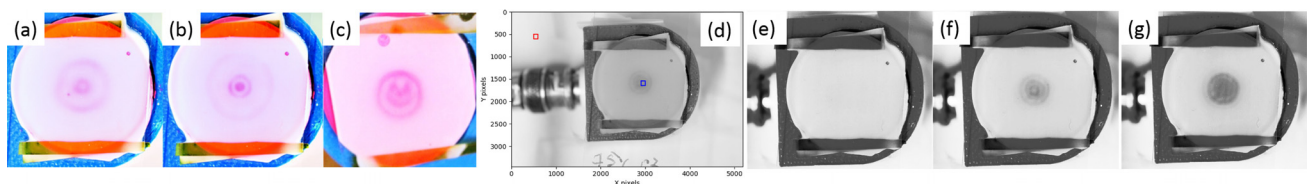

FIG. 4. Photographs of the modes taken at (a) 0.29 MHz and (b) 0.71 MHz and (c) a happy mode at 6.65 MHz. (d) The regions chosen for the ratio analysis of the 2.17 MHz mode, covering a region of clearing and a reference region. Driving voltages of (e) 50 mVpp (no clearing is visible to the eye), (f) 160 mVpp (clearing is visible), and (g) 200 mVpp (start of thermal clearing) for the 2.17 MHz mode. Note that image processing has been done to optimize for print only.

transducer surface temperature is 30 °C below the transition into the isotropic phase. Once the ultrasound is switched off, the heat takes around 60 s to dissipate, while the clearing pattern disappears within less than a second.

Displacements as small as a few nanometers are sufficient to clear the PDLC above a frequency of 1 MHz. This result is of great interest from both the physics and applications points of view. For applications, such displacements are within the range used in NDT. In terms of physics, this can shed light onto the nature of the acousto-optic effect in PDLCs. There are two possibilities for the nature: a macroscopic change in the LC droplet shape, which leads to the LC reorientation within the droplet, or microscopic flows or torques that lead to molecular realignment. The magnitude of the displacements necessary to achieve acousto-optic clearing reported here seems to rule out any macroscopic processes. Assuming a displacement of 5 nm, a film thickness of 100 μm, and an average droplet diameter of 5 μm, the deformation of each droplet would be around 0.25 nm, a change of only 5×10^{-3}%. For comparison, the individual rod-shaped molecules comprising E7 are around 1–2 nm in length. This suggests that a microscopic process is significantly more likely.

A clear dependence on frequency is observed, with lower frequencies requiring much higher displacements to clear. The curves were normalized using an S-curve fit to rescale them to cover a range from 1 (not cleared) to 0 (cleared), and the displacement that gave 50% clearing was found. This is plotted in Fig. 5(b). Two fits were performed; the $1/f$ fit would indicate a sensitivity to velocity, but a better fit is obtained from an exponential decay fit. The displacement required for 50% clearing drops to e^{-1} at around 0.75 MHz.

There are two main factors that may affect the frequency response of PDLCs and LCs: excitation wavelength vs LC droplet size and relaxation behavior of the LC. Where the excitation wavelength is much larger or much smaller than the LC droplet size, no frequency dependence is expected. For the case where the wavelength is similar to the droplet size, resonant effects may come into play. Depending on what mechanisms are responsible for the acousto-optic effect, two wavelengths are of interest: the wavelength of ultrasound in the film and the viscous wavelength.[6] The acoustic wavelength of the ultrasound inside the PDLC is calculated based on the reported speed of sound in nematics,[22,23] giving $\lambda_a \approx 2$ mm at 0.75 MHz. This is much larger than the PDLC droplet size (and even the PDLC film thickness), which rules out any resonant effects relating to the direct interaction with the acoustic wave. The viscous wave has been postulated to be generated through acoustic excitation in aligned LC layers at a rigid boundary (glass cell wall).[6] It is not clear whether the concept is applicable to PDLCs, as the geometry is different (droplets, boundaries with a soft polymer). For LC layers, the viscous wavelength is calculated using the following equation:[6]

$$\lambda_v = 2\pi \sqrt{\frac{2\eta_d}{\rho\omega}},\qquad(1)$$

where η_d is the dynamic viscosity, ρ is the density, and ω is the frequency. The viscous wavelength in E7 is $\lambda_v = 25\ \mu$m at 0.75 MHz and 7 μm at 10 MHz. For the studied frequency range, there are droplets with a size of the order of the viscous wavelength, and hence, resonant effects cannot be fully ruled out. It should be noted that the polydispersity of the PDLC film in this study is very large and may complicate or mask any resonant behavior, and the viscous wave concept may not be

applicable to PDLCs. A focused study is needed to answer questions relating to the mechanisms of the acousto-optic effect in PDLCs.

The observed frequency dependence may also be with a relaxation process. For the acousto-optic effect in aligned LCs,[24] the dynamic response suggests two relaxation mechanisms—a slow one attributed to non-uniform flows in a standing wave field and (a more pronounced) fast one attributed to a Fréedericksz-type reorientation process. Both mechanisms are of molecular level and are likely to be present in the studied PDLC. At low frequencies, there are many degrees of freedom for molecular motion (rotation) and many pathways for the input energy to be dissipated before it can realign the LC. Exciting the LC or PDLC above their relaxation frequencies will therefore result in less energy necessary to realign the LC, and therefore, the sensitivity to excitation is expected to be higher.

A dielectric relaxation associated with freezing out rotation along the short molecular axis in E7[25] and in an E7-PMMA PDLC[26] has been reported for dielectric measurements at frequencies just above 1 MHz (note that the polymer and PDLC preparation process in Ref. 26 are different from that used here). Viciosa et al. report that increasing temperature and adding a polymeric substrate shift the relaxation frequency up,[25] so a dielectric relaxation in E7 as a PDLC at 28 °C is expected to be above 1 MHz.

The acoustic frequency at which the displacement needed to change the optical properties of LCs in PDLCs drops by e is 0.75 MHz, obtained from the exponential fit to the data in Fig. 5(b). This may not be at the same frequency at which the LC's dielectric properties change, as probed by dielectric spectroscopy, even if the underlying relaxation process is the same. While the observed relaxation value is lower than expected compared to these measurements, it is of the same order of magnitude. We believe that in the current study, the observed frequency dependence can be explained by relaxation in E7. Resonant effects cannot be completely ruled out, but they are less likely.

In summary, the displacements required for the acousto-optic clearing of PDLC films (75% wt of LC, glass cover on top) are between around 2 and 50 nm, depending on the frequency of excitation. Such small displacements are around 0.005% of the film thickness and 0.05%–0.5% of the droplet size and are comparable to the molecular size of the constituents of the E7 LC mixture. Based on this value of displacement, we suggest that the observed acousto-optic effect in PDLCs is a molecular-based process rather than a macroscopic change in the droplet shape. The frequency dependence can be attributed to being primarily due to a relaxation of E7 associated with freezing out molecular rotation around the short axis. However, resonant effects related to droplet size cannot be completely ruled out. A detailed study on a monodisperse PDLC film or a similar model system is necessary to answer this question.

The displacements and ultrasonic intensities required for the acousto-optic clearing of PDLCs above 1 MHz are comparable to those used during NDT. Further optimization of the PDLC materials used would enable higher sensitivity. There is therefore significant promise for applying PDLCs as film sensors for detecting ultrasound in an NDT context.

REFERENCES

[1] J. S. Sandhu, R. A. Schmidt, and P. J. La Riviere, Med. Phys. **36**(6), 2324–2327 (2009).

[2] H. Mailer, K. L. Likins, T. R. Taylor, and J. L. Fergason, Appl. Phys. Lett. **18**, 105 (1971).

[3] S. Taniguchi, D. Koyama, Y. Shimizu, A. Emoto, K. Nakamura, and M. Matsukawa, Appl. Phys. Lett. **108**, 101103 (2016).

[4] Y. Shimizu, D. Koyama, S. Taniguchi, A. Emoto, K. Nakamura, and M. Matsukawa, Appl. Phys. Lett. **111**, 231101 (2017).

[5] Y. Shimizu, D. Koyama, M. Fukui, A. Emoto, K. Nakamura, and M. Matsukawa, Appl. Phys. Lett. **112**, 161104 (2018).

[6] O. A. Kapustina, Acoust. Phys. **54**(2), 180–196 (2008).

[7] J. S. Sandhu, R. W. Schoonover, J. I. Weber, J. Tawiah, V. Kunin, and M. A. Anastasio, Adv. Acoust. Vib. **2012**, 275858.

[8] J. W. Doane, N. A. Vaz, B. G. Wu, and S. Zumer, Appl. Phys. Lett. **48**(4), 269 (1986).

[9] D. Coates, J. Mater. Chem. **5**, 2063–2072 (1995).

[10] D. Cupelli, F. P. Nicoletta, S. Manfredi, M. Vivacqua, P. Formoso, G. DeFilpo, and G. Chidichimo, Sol. Energy Mater. Sol. Cells **93**, 2008–2012 (2009).

[11] O. A. Kapustina, Crystallogr. Rep. **59**(5), 635–649 (2014).

[12] J. V. Selinger, M. S. Spector, V. A. Greanya, B. T. Weslowski, D. K. Shenoy, and R. Shashidhar, Phys. Rev. E **66**, 051708 (2002).

[13] A. P. Malanoski, V. A. Greanya, B. T. Weslowski, M. S. Spector, J. V. Selinger, and R. Shashidhar, Phys. Rev. E **69**, 021705 (2004).

[14] Y. J. Liu, X. Ding, S. Lin, J. Shi, I.-K. Chiang, and T. J. Huang, Adv. Mater. **23**(14), 1656–1659 (2011).

[15] Y. J. Liu, M. Lu, X. Ding, E. S. P. Leong, S. Lin, J. Shi, J. H. Teng, L. Want, T. J. Bunning, and T. J. Huang, J. Lab. Autom. **18**, 291–295 (2013).

[16] O. Trushkevych, T. J. R. Eriksson, S. N. Ramadas, S. M. Dixon, and R. S. Edwards, Appl. Phys. Lett. **107**(5), 054102 (2015).

[17] J. Liu, X. Liu, and Z. Zhen, Mater. Lett. **163**, 142–145 (2016).

[18] L. Q. Zhou, G. B. Colston, M. Pearce, R. G. Prince, M. Myronov, D. R. Leadley, O. Trushkevych, and R. S. Edwards, Appl. Phys. Lett. **111**(1), 011904 (2017).

[19] A. Feeney, L. Kang, G. Rowlands, L. Q. Zhou, and S. M. Dixon, IEEE Sens. J. **19**(15), 6056–6066 (2019).

[20] P. Ronkanen, P. Kallio, M. Vilkko, and H. N. Koivo, in Micro-Nanomechatronics and Human Science, and the Fourth Symposium Micro-Nanomechatronics for Information-Based Society, Nagoya, Japan (2004), p. 313–318.

[21] T. J. R. Eriksson, S. N. Ramadas, and S. Dixon, Ultrasonics **65**, 242–248 (2016).

[22] A. V. Glushchenko, V. Sperkach, and O. Yaroshchuk, Int. J. Fluid Mech. Res. **30**(3), 299–306 (2003).

[23] M. E. Mullen, B. Luthi, and M. J. Stephen, Phys. Rev. Lett. **28**(13), 799 (1972).

[24] V. A. Greanya, A. P. Malanoski, B. T. Weslowski, M. S. Spector, and J. V. Selinger, Liq. Cryst. **32**(7), 933–941 (2005).

[25] M. T. Viciosa, A. M. Nunes, A. Fernandes, P. L. Almeida, M. H. Godinho, and M. D. Dionisio, Liq. Cryst. **29**(3), 429–441 (2002).

[26] Z. Z. Zhong, D. E. Schuele, W. L. Gordon, K. J. Adamic, and R. B. Akins, Polym. Phys. **30**(13), 1443–1449 (1992).